

Article

Low-Temperature Decomposition of Nitrous Oxide on Cs/Me_xCo_{3-x}O₄ (Me: Ni or Mg, x = 0–0.9) Oxides

Yulia Ivanova and Lyubov Isupova * 

Boreskov Institute of Catalysis, pr. Lavrentieva 5, 630090 Novosibirsk, Russia

* Correspondence: isupova@catalysis.ru

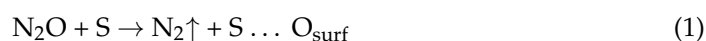
Abstract: Mixed oxides Me_xCo_{3-x}O₄ (Me: Ni or Mg, x = 0–0.9) with a spinel structure were synthesized by precipitation from Me, Co nitrate solutions using (NH₄)₂CO₃ as the precipitating agent with subsequent modification of the dry precipitate with cesium by the Pechini method and calcination. The samples were studied by XRD, TPR, and TPD methods. Their catalytic activity was studied in the low-temperature (150–350 °C) nitrous oxide decomposition process. It was shown that an increase in the degree of substitution of cobalt (x) leads to a significant decrease in the degree of crystallization of the oxides, an increase in the specific surface area, and the formation of surface weakly bound oxygen species. The highest activity was shown by the catalysts with a degree of substitution x = 0.1, especially by the nickel-substituted sample, which contained the maximum amount of weakly bound surface oxygen species. The difference in the influence of Mg and Ni on the Me_xCo_{3-x}O₄ properties is discussed.

Keywords: substituted cobalt spinel; nitrous oxide decomposition; loosely bound oxygen species

1. Introduction

Nitrous oxide (N₂O) is a greenhouse gas that has a high global warming factor, 310 times more than CO₂; thus, reducing N₂O emissions is the current trend. Among various methods for removing nitrous oxide, the most interesting is the method of catalytic decomposition. One of the largest suppliers of N₂O to the atmosphere is the production of nitric acid. The nitric acid production flow sheet includes several abatement methods/possibilities to reduce N₂O emissions. Tertiary abatement measures of N₂O removal after the absorber have great advantages because they do not affect the axial flow of nitric acid production, using a selective catalytic reduction (SCR) block with ammonia for de-NO_x [1]. However, for implementation under reactor conditions, an SCR system requires a low-temperature catalyst. It is desirable that the de-N₂O catalyst for the combined exhaust gas treatment system should work in the low-temperature range of 200–300 °C and be resistant to inhibitors like O₂ and H₂O. The range of catalytic systems for the low-temperature decomposition of N₂O is wide [2,3] and includes platinum subgroup metals (Ru, Rh, Pd, Ir, and Pt), oxides of elements of the rare earth subgroup, and oxides of transition d-elements (in particular, Cu, Ni, Co, and Fe). Many catalytic systems containing noble metals and elements of the rare earth subgroup are deactivated in the presence of inhibitors and have a high cost, which makes it difficult to use them as the exhaust gas purification catalysts.

The catalytic decomposition of N₂O (de-N₂O) implies that as a result, environmentally neutral molecules of N₂ and O₂ will be formed. The decomposition of N₂O is an irreversible exothermic reaction. It proceeds by two mechanisms: the Langmuir–Hinshelwood (L–H) mechanism characterized by low activation energy of the stage of surface oxygen diffusion and recombination (stage 1) and the Eley–Rideal (E–R) mechanism characterized by high activation energy of surface diffusion, which requires large amounts of energy for oxygen diffusion (stage 3) [4–6]:



Citation: Ivanova, Y.; Isupova, L. Low-Temperature Decomposition of Nitrous Oxide on Cs/Me_xCo_{3-x}O₄ (Me: Ni or Mg, x = 0–0.9) Oxides. *Catalysts* **2023**, *13*, 137. <https://doi.org/10.3390/catal13010137>

Academic Editors: Małgorzata Rutkowska and Lucjan Chmielarz

Received: 12 December 2022

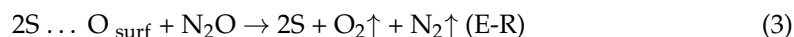
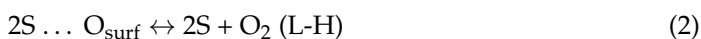
Revised: 30 December 2022

Accepted: 4 January 2023

Published: 6 January 2023



Copyright: © 2023 by the authors. Licensee MDPI, Basel, Switzerland. This article is an open access article distributed under the terms and conditions of the Creative Commons Attribution (CC BY) license (<https://creativecommons.org/licenses/by/4.0/>).



where S is the active site of the surface, and S ... O_{surf} is the oxygen adsorbed on the active site of the surface. For various oxide systems, stages (2) and (3) were found to be relatively slow compared to stage (1). In other words, O₂ desorption can be considered the rate-determining stage of the catalytic decomposition of N₂O regardless of the mechanism of O₂ formation. To date, the spinel-like structure of Co₃O₄ oxide, as well as the related binary substituted oxides, have proved to be the most promising candidates for de-N₂O due to the redox ability of cobalt cations, a high concentration of oxygen vacancies, and a weak Co-O bond [7,8]. The substitution of Co cations in certain positions of the spinel oxide matrix has a significant effect on the binding energy of the active center with oxygen. The highest rates of activity in the decomposition reaction of N₂O were demonstrated by magnesium- and nickel-substituted Co₃O₄ spinels. The incorporation of Ni²⁺ or Mg²⁺ into the Co₃O₄ structure promotes better desorption of O₂ and lowers the temperature of de-N₂O [9–14]. Both cations can displace cobalt not only in the tetrahedral environment, but also to some extent in the octahedral one [15,16]. This leads to structural distortions with an increase in the bond lengths in octahedra and a decrease in tetrahedra. The effect is more pronounced for nickel-substituted Co₃O₄ spinels, and to a lesser extent for magnesium-substituted ones.

Surface modification of Co₃O₄ spinels with alkali metal cations makes them more active and resistant to inhibitors. The beneficial effect of different alkali promoters on the Co₃O₄ activity in nitrous oxide decomposition increases in the following order: Li ≪ Na < Rb ≅ K < Cs [17,18], which is consistent with a decrease in the electronegativity values from Li to Cs [19]. Most of the studies on the influence produced by the nature of the alkaline modifier and its precursors were carried out mainly for pure Co₃O₄ spinel. However, it cannot be ruled out that surface modification with alkali cations of substituted M_xCo_{3-x}O₄ (Me = Mg, Ni) spinels may also change their catalytic activity and stability.

In this work, Me_xCo_{3-x}O₄ (Me: Ni or Mg, x = 0–0.9) oxides were prepared by the coprecipitation method. The samples were further modified with Cs cations according to the Pechini method. The influence of the catalyst composition on the catalytic activity and stability to inhibitors (oxygen, water vapor) in N₂O decomposition was revealed.

2. Results and Discussion

2.1. XRD Study of Samples

Figure 1 shows X-ray diffraction patterns of the prepared 2%Cs/Ni_xCo_{3-x}O₄ (Cs/Ni-Co) and 1%Cs/Mg_xCo_{3-x}O₄ (Cs/Mg-Co) (x = 0–0.9) samples. The samples are well crystallized spinels (Fd-3m) [20] typical of Co₃O₄, and it is in good agreement with the available database (ICSD №69365). Table 1 lists the calculated parameters of crystal cells of the substituted cobalt spinels for the samples.

An increase in the Mg or Ni content leads to an increase in the lattice parameters and a decrease in the CSR (coherent scattering region) size, which is more pronounced in the case of Mg. On the X-ray diffraction patterns of Cs/Ni-Co (x = 0.5 and 0.9) samples, along with the peaks related to spinel, a reflection is additionally observed in the region of 2θ = 43.37, which refers to the NiO impurity phase. For Cs/Mg-Co samples, the formation of the magnesium oxide phase is not observed. The substitution with Mg or Ni leads also to an increase in S_{BET} values of the samples (Table 1). In the case of substitution with Ni, the CSR size changes nonmonotonically with increasing the degree of substitution, as does S_{BET}. This can be attributed to the fact that a part of the nickel is not a part of the spinel but exists in the NiO impurity phase, while the formation of a continuous series of homogeneous solid solutions for the Cs/Mg-Co samples may be proposed [21].

According to [22], the formation of a normal spinel, where only Co²⁺ cations are substituted, should not lead to an increase in the lattice parameter since the radii of the Ni²⁺ (0.69 Å), Mg²⁺ (0.72 Å) and Co²⁺ (0.74 Å) cations are very close [23]. An increase in cell parameters with substitution degree indicates that both the cobalt and nickel

cations may occupy both the octahedral and tetrahedral positions. The inversion in both systems is in agreement with the literature data [22–25]. Based on the presented data, $\text{Mg}_x\text{Co}_{3-x}\text{O}_4$ and $\text{Ni}_x\text{Co}_{3-x}\text{O}_4$ oxides are mostly the inverse spinels in which an increase in x leads to an increase in the length of octahedral bonds and a shortening of tetrahedral ones [14,15,24–27]. In [26], it was shown that as the spinel inversion increases, the lattice parameters can also increase.

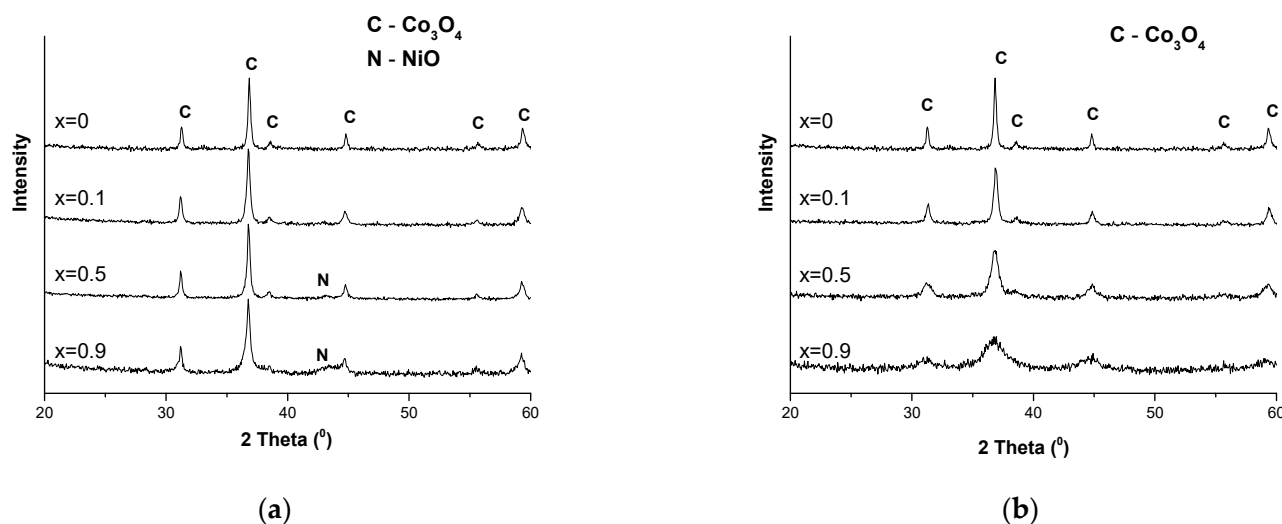


Figure 1. XRD patterns of samples: (a) Cs/Ni-Co; (b) Cs/Mg-Co.

Changes in the structural parameters and S_{BET} in both substituted spinel systems Cs/Mg-Co and Cs/Ni-Co depend on the nature and amount of the modifying Ni or Mg cations. Thus, an increase in the lattice parameter of the prepared substituted spinels indicates their partial inversion.

Table 1. Physicochemical characteristics of the $\text{Cs}/\text{Me}_x\text{Co}_{3-x}\text{O}_4$ (Me: Ni or Mg, $x = 0\text{--}0.9$) samples and the half-transformation temperature (T_{50}).

x	Phase Composition	Lattice Parameter, Å	CSR, Å	S_{BET} , m^2/g	T_{50} , °C
0	Spinel	8.083	380	12	275
Cs/Ni-Co					
0.1	Spinel	8.088	260	32	196
0.5	Spinel, NiO	8.094	310	23	224
0.9	Spinel, NiO	8.101	280	26	250
Cs/Mg-Co					
0.1	Spinel	8.084	210	36	210
0.5	Spinel	8.091	120	57	257
0.9	Spinel	8.099	45	144	220

2.2. H_2 -TPR and O_2 -TPD Study of Samples

The temperature-programmed reduction (H_2 -TPR) curves of the samples show two hydrogen uptake peaks (Figure 2a). The authors of [28,29] attribute the low-temperature peak to the reduction of Co^{3+} to Co^{2+} , and the high-temperature peak to the reduction of Co^{2+} to Co^0 .

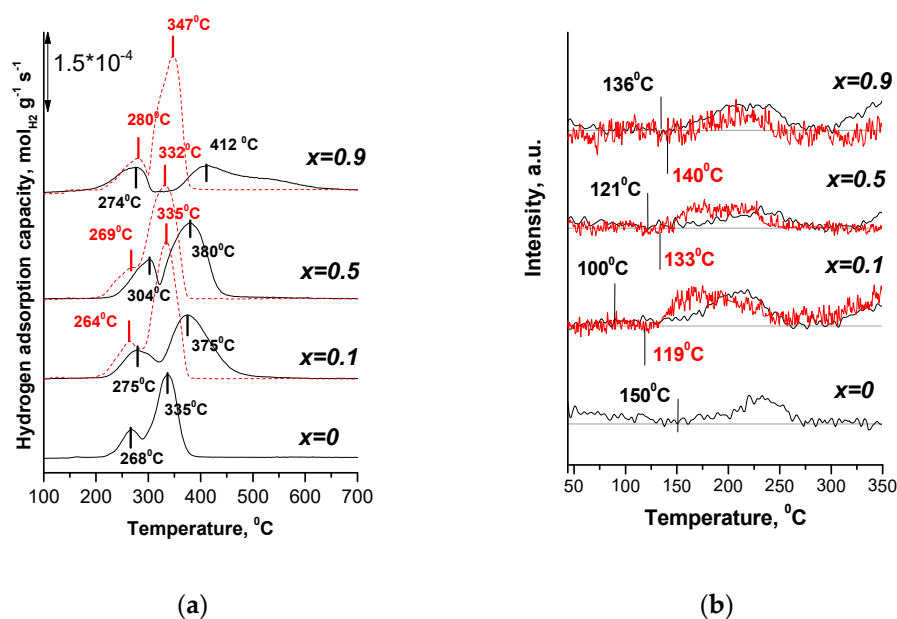


Figure 2. Profiles of the Cs/Mg-Co (black) and Cs/Ni-Co (red) samples obtained by (a) H₂-TPR and (b) O₂-TPD.

The substitution of cobalt cations with Ni/Mg cations lowers the initial reduction temperature (T_0^{TPR}) (Table 2). The temperatures of the reduction maxima corresponding to the gradual reduction of cobalt cations $\text{Co}^{3+} \rightarrow \text{Co}^{2+} \rightarrow \text{Co}^0$ were 268 and 335 °C, respectively, for the ($x = 0$) sample. These data are consistent with those reported in [28,29]. The reduction maxima of the low-temperature peaks for the substituted spinels shift insignificantly. In this case, the introduction of nickel leads to a decrease in the temperature of the maximum, and magnesium—to an increase. The shift of the maxima to the high-temperature region is most pronounced for the Cs/Mg-Co samples, but it virtually does not occur for the Cs/Ni-Co samples. According to the literature data for $\text{Ni}_x\text{Co}_{3-x}\text{O}_4$ [30,31], the temperature peaks at 221 and 284 °C correspond to the reduction of Ni^{3+} to Ni^{2+} and Co^{3+} to Co^{2+} , respectively. As the temperature further increases, the reduction of Ni^{2+} to Ni^0 and Co^{2+} to Co^0 proceeds at the temperatures of 335 and 374 °C, respectively [30,31]. The authors of [21] state that depending on the CoO/MgO ratio, either (MgCo)O or MgCo_2O_4 solid solution can be formed. The reduction temperature of said compounds varies in the range of 500–1000 °C. Hence, it follows that the introduction of nickel has little effect on the reduction temperature of Cs/Ni-Co samples, while the introduction of magnesium increases the reduction temperature of Cs/Mg-Co samples and produces the particularly high temperature peaks. The increase in x leads to an increase in the octahedral bond lengths ($\text{Me}^{3+}\text{-O}$) and a shortening of the tetrahedral ($\text{Me}^{2+}\text{-O}$) ones [15]. This behaviour reflects the revealed cation distributions. The octahedra grow because of the increasing amount of larger divalent cations residing there. The smaller Co^{3+} cations displaced by them enter the tetrahedral sites and the tetrahedral bond lengths decrease. Nickel in the lower degrees of substitution tends to occupy octahedral centers much more strongly than magnesium [15]. This may explain the greater increase in the lattice parameter and the decrease in the reduction temperature for the Cs/Ni-Co ($x = 0.1$) sample. The total amount of hydrogen consumed for the reduction of the Cs/ Co_3O_4 sample is close to the theoretically calculated one, 16.6×10^{-3} mol/g (Table 2). The total amount of hydrogen consumption decreases with an increase in the degree of substitution, the exception is the sample Cs/Ni-Co ($x = 0.1$). The value of hydrogen consumption in the first peak changes through a maximum in the degree of substitution ($x = 0.1$) for both series. Probably the increase in the absorption in the first peak for the ($x = 0.1$) samples is due to an increase in the content of $\Sigma(\text{Co}+\text{Me})^{3+}$. In the second peak, the amount of absorbed hydrogen should be proportional to the amount of divalent cations, since the reduction of 1 mol of

$\Sigma(\text{Co} + \text{Me})^{2+}$ accounts for 1 mol of H_2 . The amount of absorbed hydrogen in the second peak for the Cs/Ni-Co ($x = 0.1$) sample exceeds the calculated amount of cations in the substituted samples $\Sigma(\text{Co} + \text{Me})^{2+} = 12.5 \times 10^{-3}$ mol/g for a normal spinel. Therefore, the reduction of $\Sigma(\text{Co} + \text{Me})^{3+}$ for Cs/Ni-Co ($x = 0.1$) samples at low temperatures is not complete and continues at high temperatures, thus contributing to the absorption of H_2 in the second peak. This means that the actual amount of $\Sigma(\text{Co} + \text{Me})^{3+}$ in the ($x = 0.1$) sample is greater than that calculated from the first peak. Thus, nickel is more prone to inversion. For the Cs/Mg-Co samples, the amount of absorbed H_2 in the second peak does not exceed the calculated amount of $\Sigma(\text{Co} + \text{Me})^{2+}$; therefore, it reflects only the reduction of divalent cations. Thus, Cs/Ni-Co samples are more easily reduced by hydrogen and are more enriched in $\Sigma(\text{Co} + \text{Me})^{3+}$ (taking into account that not all of them are restored in the first peak) than Cs/Mg-Co samples, especially in a low degree of substitution ($x = 0.1$).

According to the O_2 -TPD data, the oxygen desorption occurs in two stages in a wide temperature range of 80–500 °C (Figure 2b). Considering the conditions of N_2O decomposition in the SCR reactor, the low-temperature desorption peak is of the greatest interest. The initial temperature of O_2 desorption (T_0^{TPD}) for Cs/ Co_3O_4 is 150 °C. The substitution of cobalt cations with Ni or Mg cations reduces the initial desorption temperature (T_0^{TPD}) in substituted Cs/Ni-Co and Cs/Mg-Co samples (Table 2). The presence of Mg in the samples reduces (T_0^{TPD}) more than Ni. The amount of desorbed oxygen varies through the maximum for both series at ($x = 0.1$), but is more pronounced for Cs/Ni-Co. At low temperatures, the main contribution to oxygen desorption is made by weak physical forces, for which an important role is played by the electronic interaction of the surface atoms of the catalyst, including Mg or Ni modifiers. The lower electronegativity of magnesium makes it possible to subsidize the electron density and reduce the energy of oxygen desorption. However, it is shown that a greater amount of desorbed oxygen in the Cs/Ni-Co samples is observed at relatively lower S_{BET} values than in the Cs/Mg-Co samples. This leads to the imperfection of the oxygen sublattice and the formation of structural defects on which weakly-bound oxygen species are adsorbed. It is possible that this is the effect of a larger amount of applied cesium in the Cs/Ni-Co series. The O_2 -TPD findings correlate with the H_2 -TPR observations.

Table 2. H_2 -TPR temperatures of the initial reduction and H_2 consumption. The amount of desorbed oxygen by O_2 -TPD and the initial desorption temperatures.

x	$T_0^{\text{TPR}}, \text{ }^\circ\text{C}$	$\Sigma\text{H}_2 \times 10^{-3},$ mol/g	$\text{H}_2 \times 10^{-3},$ mol/g $\text{Co}^{3+} \rightarrow \text{Co}^{2+}$	$\text{H}_2 \times 10^{-3},$ mol/g $\text{Co}^{2+} \rightarrow \text{Co}^0$	$T_0^{\text{TPD}},$ °C	$\Sigma\text{O} \times 10^{17},$ at/m ²
0	212	16.6	4.0	12.6	150	3.3
			Cs/Ni-Co			
0.1	188	17.1	4.2	12.9	119	4.2
0.5	200	15.7	3.3	12.4	133	3.9
0.9	207	15.5	3.5	12.0	140	1.2
			Cs/Mg-Co			
0.1	200	16.1	4.2	11.9	100	3.4
0.5	207	15.6	4.0	11.6	121	1.2
0.9	188	13.2	3.8	9.4	136	0.8

2.3. Catalytic Activity

2.3.1. Dependence of Activity on the Content of Cs

A study on the catalytic activity of Co spinel samples with a degree of substitution ($x = 0.5$) of Mg or Ni cations showed that when the cesium content varied from 0 to 3 wt%, samples containing 1–2 wt% Cs demonstrated high performance (Figure 3).

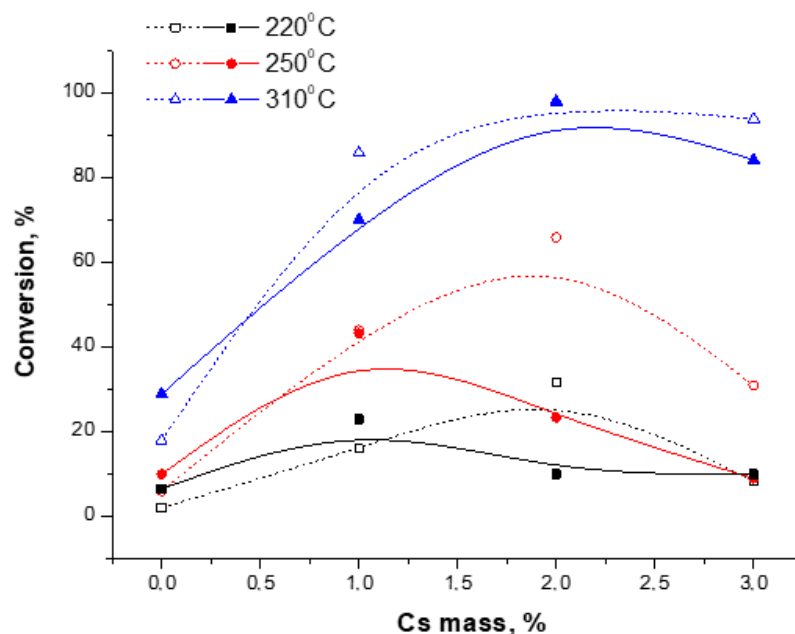


Figure 3. Influence of the mass content of Cs cations on N₂O conversion in the temperature range 220–310 °C. Samples: Ni_{0.5}Co_{2.5}O₄ (dotted) and Mg_{0.5}Co_{2.5}O₄ (solid).

It was shown that at low temperatures of 220–250 °C, the optimal content is 1 wt% Cs for Mg_{0.5}Co_{2.5}O₄ and 2 wt% Cs for Ni_{0.5}Co_{2.5}O₄. The authors of [32] estimated the optimal content of potassium cations for the Co_{2.6}Zn_{0.4}O₄ catalyst in the range of 2–6 atoms of K/nm². According to [18,33], for the Co₃O₄ catalyst the optimal amount of Cs is 2–3 at. Cs/nm² (i.e., ~1 wt% Cs). In our case, the amount of the alkaline promoter does not correlate with the parameters (S_{BET}) of the samples: Mg_{0.5}Co_{2.5}O₄~1 at. Cs/nm² (1 wt% Cs) and for Ni_{0.5}Co_{2.5}O₄~4 at. Cs/nm² (2 wt% Cs). Thus, for a sample containing Ni, the mass content of Cs is two times higher despite the ~2.5 times smaller specific surface area compared to a sample containing Mg (Table 1). This can be explained by the lower Pauling electronegativity for Mg (0.65) in contrast to Ni (0.69), which further enhances the action of alkali metal cations. The low ionization energy of alkali metal cations allows them to easily form a bond with oxygen adsorbed on the surface of the catalyst, promoting the recombination of active centers of N₂O decomposition [34]. Magnesium, unlike nickel, is the main donor of electron density. The properties of alkaline earth metal cations are close to alkaline, which causes a decrease in the concentration of Cs as a promoter for Mg_{0.5}Co_{2.5}O₄.

Based on the data obtained, a series of Cs/Mg-Co samples was modified with 1 wt% Cs, and a series of Cs/Ni-Co samples—with 2 wt% Cs.

2.3.2. The Decomposition of N₂O

A study on the catalytic activity of Cs/Mg-Co and Cs/Ni-Co samples with cobalt substitution degrees ($x = 0-0.9$) in a model mixture containing 0.15% N₂O in helium showed that high conversion values were demonstrated by samples with the ($x = 0.1$) substitution degree (Figure 4).

The half-transformation temperature (T_{50}) for samples with the degree of substitution ($x = 0.1$) is minimal and amounts to 196 and 210 °C for Cs/Ni-Co and Cs/Mg-Co, respectively (Table 1). For unsubstituted cobalt spinel Co₃O₄, this value is maximal and amounts to 275 °C. High specific activity (the activity normalized per m², the reaction rate) was demonstrated by Cs/Ni-Co ($x = 0.1$ and 0.5) and Cs/Mg-Co ($x = 0.1$) samples (Figure 4b). The Cs/Mg-Co sample with ($x = 0.1$) is inferior to the Cs/Ni-Co samples ($x = 0.1$ and 0.5) in the reaction rate and in the amount of desorbed oxygen referred to the surface area. The observed correlation indicates a significant effect of weakly bound surface oxygen in the

catalysts on the reaction rate, which is consistent with the data on the rate-limiting stage of this reaction at low temperatures [4,5].

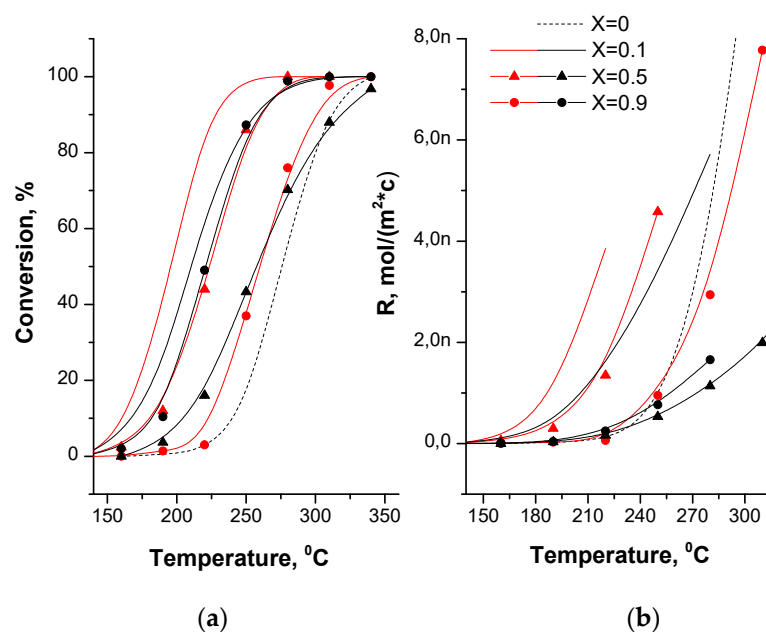


Figure 4. Temperature dependence of (a) conversion and (b) reaction rate of N_2O decomposition for Cs/Mg-Co (black) and Cs/Ni-Co (red) samples.

2.3.3. The Decomposition of N_2O in the Presence of Inhibitors

Under the actual conditions of the SCR reactor, the tail gases from the production of nitric acid, in addition to nitrous oxide, contain oxygen and water vapor [5]. The effect of inhibitors (H_2O , O_2) was tested on samples with high activity in the decomposition of pure nitrous oxide Cs/Ni-Co and Cs/Mg-Co with the degree of substitution ($x = 0.1$). The data obtained indicate a decrease in the catalyst activity in the presence of inhibitors in the reaction mixture (Figure 5). Samples Cs/Ni-Co and Cs/Mg-Co ($x = 0.1$) lose their activity during the first two hours in the reaction mixture of 1500 ppm N_2O in He (without inhibitors), nitrous oxide conversion for Cs/Ni-Co decreases by $\sim 15\%$ and for Cs/Mg-Co by $\sim 7\%$. In the presence of inhibitors (H_2O , O_2), the initial activity of the samples is lower than in their absence, but there is a tendency to lose activity in the first hours. The loss of activity was $\sim 25\%$ for Cs/Ni-Co and $\sim 10\%$ for Cs/Mg-Co. In this case, the unmodified Cs/ Co_3O_4 catalyst loses $\sim 40\%$ of its activity in the presence of inhibitors. Long-term tests revealed a higher stability of the Cs/Mg-Co sample as compared to Cs/Ni-Co. A similar effect of stronger inhibition on the $Ni_{0.74}Co_{0.26}Co_2O_4$ catalyst than on $Mg_{0.54}Co_{0.46}Co_2O_4$ was observed in [9]. The authors of [9,35–37] showed a stronger inhibition of substituted Co spinels by water rather than by oxygen.

A comparison of the N_2O conversion and the specific activity of Cs/Ni-Co and Cs/Mg-Co samples shows that their activity increases not only due to an increase in S_{BET} , but mainly due to an increase in the number of weakly bound oxygen centers of the samples. The Cs/Ni-Co ($x = 0.1$) sample was characterized by the maximum values of oxygen desorption according to O_2 -TPD and H_2 -TPR data and had high conversion and specific activity normalized to the specific surface area value. The high activity of the Cs/Ni-Co ($x = 0.1$) sample is due to a large number of weakly bound oxygen centers. The same active sites interact with inhibitors, which leads to rapid deactivation of the Cs/Ni-Co ($x = 0.1$) sample compared to Cs/Mg-Co ($x = 0.1$). The deactivation of both samples in the presence of inhibitors or without them proceeds in the first ~ 2 h.

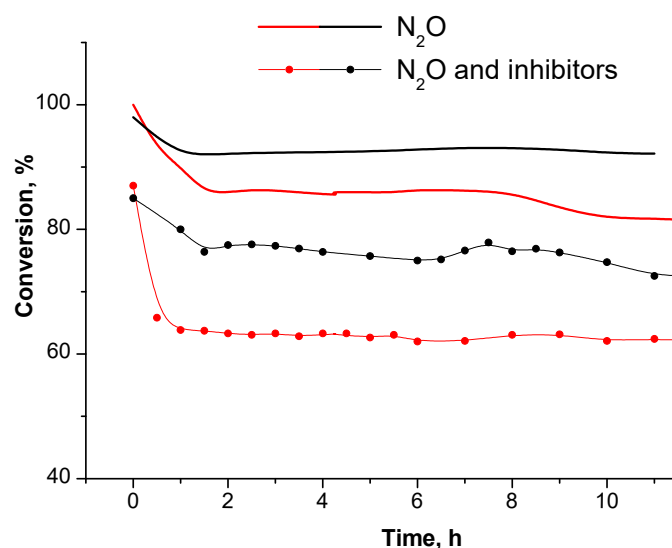


Figure 5. The N_2O conversion during testing of the Cs/Mg-Co (black) and Cs/Ni-Co (red) ($x = 0.1$) samples at 300 °C.

3. Experimental

3.1. Samples Preparation

Cs/Me_xCo_{3-x}O₄ ($x = 0-0.9$, Me = Mg, Ni) samples were synthesized by coprecipitation. Short designations for the samples are Cs/Mg-Co and Cs/Ni-Co, respectively. For the synthesis, Ni(NO₃)₂·6H₂O or Mg(NO₃)₂·6H₂O and Co(NO₃)₂·6H₂O aqueous solutions were used in the stoichiometric ratio of cations required to obtain a mixed spinel of a given composition. Precipitation was implemented at room temperature and a pH of 8–8.5 using (NH₄)₂CO₃ as the precipitating agent. The resulting precipitates were filtered off, washed to a pH of 7 and dried at 120 °C for 10 h. The dried precipitates were modified with cesium by impregnation from a solution containing CsNO₃, ethylene glycol, and citric acid (the Pechini method). The Cs/Mg-Co samples were modified with 1 wt% Cs; the Cs/Ni-Co samples and the Cs/Co₃O₄ sample were modified with 2 wt% Cs. All the samples were calcined for 2 h at a temperature of 450 °C.

3.2. Catalysts Characterization

The phase composition of the samples was determined by X-ray diffraction (XRD) analysis on a Bruker D8 diffractometer using CuK α radiation ($\lambda = 1.5418 \text{ \AA}$). The samples were scanned point-by-point with 0.05° increments in a 2 θ range of 20–60°. The structural parameters were calculated using the FullProf software. The specific surface area (S_{bet} , m²/g) was measured by argon sorption at –196 °C, followed by thermal desorption, at four points of the sorption equilibrium with a SORBI m 4.1 device (ZAO META) using the Sorbi m Version 4.2 software. Helium was used as a carrier gas. The values of S_{bet} were calculated by the Brunauer–Emmett–Teller method (BET). The samples with the grain size of 0.25–0.50 μm were studied by a temperature programmed reduction with hydrogen (H₂-TPR) in a flow unit equipped with a thermal conductivity detector for a catalyst fraction of 0.25–0.50 mm. A weighed sample (10 mg) was subjected to preliminary holding in argon at 200 °C for 30 min and subsequent cooling in argon to room temperature, and then reduced in a mixture (10% H₂ in argon) at a flow rate of 40 mL/min. The samples were heated to 900 °C at a rate of 10 deg/min. Studies of the samples by temperature programmed desorption of oxygen (O₂-TPD) were conducted in a flow unit. The mixture at the outlet of the reactor was analyzed using a QMS 100 mass spectrometer (Stenford Research Systems, SRS). The samples were pretreated in a mixture of 20% O₂ in He at 450 °C for 60 min and then cooled to room temperature. The weighed portion of the sample was 200 mg; the feed flow rate of He was 3.6 L/h. The samples were heated to 450 °C at a rate of 10 °C/min.

3.3. Activity Tests

The catalytic activity in de-N₂O reaction was studied in a flow tube reactor (5 mm inner diameter) at 130–430 °C, ambient pressure, and a space velocity (GHSV) of 9000 h⁻¹. Standard tests were carried out using the reaction mixture of 1500 ppm N₂O in He. Stability experiments were carried out in a gas mixture of 3% O₂ or 2.5–3% H₂O at a temperature of 250 °C. Reactant and product concentrations were analyzed by a Fourier transform IR spectrometer FT-801. The conversion of N₂O was calculated by the following equation:

$$X_{N_2O} = \frac{C_{N_2O}^{decomp}}{C_{N_2O}^{feed}} \times 100\%,$$

where $C_{N_2O}^{decomp}$ is the decomposed gas concentration and $C_{N_2O}^{feed}$ is the feed gas concentration. The rate was determined under the assumption of a first-order reaction by the following equation:

$$R_{N_2O} = \frac{UN_A}{mS_{sp}} \ln \frac{1}{(1-x)} \text{ [mol m}^{-2} \text{ s}^{-1}\text{]},$$

where U is the flow rate of the reaction mix [mol/s]; N_A is the Avogadro constant; m is the weight [g]; S_{sp} is the specific surface area [m²/g], and x is the fraction of converted N₂O.

The temperature at which the N₂O conversion was 50% (denoted as T₅₀—the half-life temperature of nitrous oxide) was a measure of the catalyst activity.

4. Conclusions

A series of 1%Cs/Mg_xCo_{3-x}O₄ and 2%Cs/Ni_xCo_{3-x}O₄ oxide catalysts with the degree of substitution ($x = 0-0.9$) prepared by precipitation route and promoted with Cs had the spinel structure typical of Co₃O₄. The change in the structural parameters and S_{bet} in both series depends on the nature and amount of modifying Ni or Mg cations. The observed increase in the lattice parameters of substituted spinels in both series indicates their partial inversion.

Evaluation of the influence of the promoter on the activity of substituted spinels for ($x = 0.5$) samples showed that the optimal amount of the promoter depends on the nature of the substituting cation. The optimal amount of alkaline promoter for the samples containing Mg was determined as 1 wt% Cs, while for the samples containing Ni, as 2 wt% Cs.

2%Cs/Ni_{0.1}Co_{2.9}O₄ samples are more easily reduced with hydrogen (H₂-TPR) than 1%Cs/Mg_{0.1}Co_{2.9}O₄ samples and contain a large quantity of weakly bound oxygen species according to O₂-TPD and H₂-TPR. 1%Cs/Mg_{0.1}Co_{2.9}O₄ and 2%Cs/Ni_{0.1}Co_{2.9}O₄ samples with the degree of substitution ($x = 0.1$) showed the highest conversion degrees in the series in N₂O decomposition, which correlates with H₂-TPR and H₂-TPD data. Therewith, the 2%Cs/Ni_{0.1}Co_{2.9}O₄ samples ($x = 0.1$ and 0.5) had a higher specific activity as compared to the 1%Cs/Mg_{0.1}Co_{2.9}O₄ samples. The activity increases mainly due to the large number of weakly bound oxygen species.

Under the conditions of a SCR reactor, the 1%Cs/Mg_{0.1}Co_{2.9}O₄ sample is of the greatest interest for application as the second layer of the catalyst for the decomposition of nitrous oxide, taking into account the resistance of the samples to the reaction medium.

Author Contributions: Y.I.—methodology, conceptualization, validation, and investigation; L.I.—supervision, methodology. All authors have read and agreed to the published version of the manuscript.

Funding: This work was supported by the budget project AAAA-A21-121011490008-3 for the Boreskov Institute of Catalysis.

Data Availability Statement: Informed consent was obtained from all subjects involved in the study.

Conflicts of Interest: The authors declare no conflict of interest.

References

1. Chumachenko, V.A.; Isupova, L.A.; Ivanova, Y.A.; Ovchinnikova, E.V.; Reshetnikov, S.I.; Noskov, A.S. Technologies for Simultaneous Low-Temperature Catalytic Removal of NO_x and N₂O from the Tail Gases of Nitric Acid Plants. *Chem. Sustain. Dev.* **2020**, *28*, 203–212. [CrossRef]
2. Isupova, L.A.; Ivanova, Y.A. Removal of nitrous oxide in nitric acid production. *Kinet. Catal.* **2019**, *60*, 744–760. [CrossRef]
3. Konsolakis, M. Recent advances on nitrous oxide (N₂O) decomposition over non-noble metal oxide catalysts: Catalytic performance, mechanistic considerations and surface chemistry aspects. *ACS Catal.* **2015**, *5*, 6397–6421. [CrossRef]
4. Yu, H.; Wang, X. Apparent activation energies and reaction rates of N₂O decomposition via different routes over Co₃O₄. *Catal. Commun.* **2018**, *106*, 40–43. [CrossRef]
5. Kapteijn, F.; Marban, G.; Rodriguez-Mirasol, J.; Moulijn, J.A. Kinetic Analysis of the Decomposition of Nitrous Oxide over ZSM-5 Catalysts. *J. Catal.* **1997**, *167*, 256–265. [CrossRef]
6. Dandl, H.; Emig, G. Mechanistic approach for the kinetics of the decomposition of nitrous oxide over calcined hydrotalcites. *Appl. Catal. A Gen.* **1998**, *168*, 261–268. [CrossRef]
7. Ma, Z.; Ren, Y.; Lu, Y.B.; Peter, P.G. Catalytic decomposition of N₂O on ordered crystalline metal oxides. *J. Nanosci. Nanotechnol.* **2013**, *13*, 5093–5103. [CrossRef]
8. Hu, X.; Wang, Y.; Wu, R.; Zhao, Y. Graphitic carbon nitride-supported cobalt oxides as a potential catalyst for decomposition of N₂O. *Appl. Surf. Sci.* **2021**, *538*, 14815. [CrossRef]
9. Yan, L.; Ren, T.; Wang, X.; Ji, D.; Suo, J. Catalytic decomposition of N₂O over M_xCo_{1-x}Co₂O₄ (M = Ni, Mg) spinel oxides. *Appl. Catal. B* **2003**, *45*, 85–90. [CrossRef]
10. Liu, Z.; He, F.; Ma, L.; Peng, S. Recent Advances in Catalytic Decomposition of N₂O on Noble Metal and Metal Oxide. *Catal. Catal. Surv. Asia* **2016**, *20*, 121–132. [CrossRef]
11. Zheng, L.; Li, H.J.; Xu, X.F. Catalytic decomposition of N₂O over Mg-Co composite oxides hydrothermally prepared by using carbon sphere as template. *J. Fuel Chem. Technol.* **2018**, *46*, 569–577. [CrossRef]
12. Zhang, H.J.; Jian, W.; Xu, X.F. Catalytic decomposition of N₂O over Ni_xCo_{1-x}CoAlO₄ spinel oxides prepared by sol-gel method. *J. Fuel Chem. Technol.* **2015**, *43*, 81–87. [CrossRef]
13. Russo, N.; Fino, D.; Saracco, G.; Specchiaet, V. N₂O catalytic decomposition over various spinel-type oxides. *Catal. Today* **2007**, *119*, 228–232. [CrossRef]
14. Abu-Zied, B.M.; Soliman, S.A.; Abdallah, S.E. Pure and Ni-substituted Co₃O₄ spinel catalysts for direct N₂O decomposition. *Chin. J. Catal.* **2014**, *35*, 1105–1112. [CrossRef]
15. Krezhov, K.; Konstantinov, P. Cationic distributions in the binary oxide spinels M_xCo_{3-x}O₄ (M = Mg, Cu, Zn, Ni). *Physica B* **1997**, *234–236*, 157–158. [CrossRef]
16. Krezhov, K.; Konstantinov, P. On the cationic distribution in Mg_xCo_{3-x}O₄ spinels. *J. Phys. Condens. Matter* **1992**, *4*, 543–548. [CrossRef]
17. Wójcik, S.; Grzybek, G.; Stelmachowski, P.; Sojka, Z.; Kotarba, A. Bulk, Surface and Interface Promotion of Co₃O₄ for the Low-Temperature N₂O Decomposition Catalysis. *Catalysts* **2020**, *10*, 41. [CrossRef]
18. Stelmachowski, P.; Maniak, G.; Kotarba, A.; Sojka, Z. Strong electronic promotion of Co₃O₄ towards N₂O decomposition by surface alkali dopants. *Catal. Commun.* **2009**, *10*, 1062–1065. [CrossRef]
19. Maniak, G.; Stelmachowski, P.; Kotarba, A.; Sojka, Z.; Rico-Pérez, V.; Bueno-López, A. Rationales for the selection of the best precursor for potassium doping of cobalt spinel based deN₂O catalyst. *Appl. Catal. B Environ.* **2013**, *136–137*, 302–307. [CrossRef]
20. Rashmirekha, S.; Barsha, D.; Chinmaya, K.S.; Kali, S.; Tondepur, S.; Gamini, S.; Manickam, M. Influence of Synthesis Temperature on the Growth and Surface Morphology of Co₃O₄ Nanocubes for Supercapacitor. *Appl. Nanomater.* **2017**, *7*, 356. [CrossRef]
21. Wang, H.Y.; Ruckenstein, E. CO₂ reforming of CH₄ over Co/MgO solid solution catalysts—Effect of calcination temperature and Co loading. *Appl. Catal. A Gen.* **2001**, *209*, 207–215. [CrossRef]
22. Markov, L.; Petrov, K. Nickel-cobalt oxide spinels prepared by thermal decomposition of nickel(II)-cobalt(II) hydroxide nitrates. *React. Solids* **1986**, *1*, 319–327. [CrossRef]
23. Shannon, R.D. Revised effective ionic radii and systematic studies of interatomic distances in halides and chalcogenides. *Acta Cryst.* **1976**, *A 32*, 751–767. [CrossRef]
24. Lenglet, M.; Guillet, R.; Dürr, J.; Gryffroy, D.; Vandenberghe, R.E. Electronic structure of NiCo₂O₄ by XANES, EXAFS and ⁶¹Ni Mössbauer studies. *J. Solid State Commun.* **1990**, *74*, 1035–1039. [CrossRef]
25. Iliev, M.N.; Silwal, P.; Loukya, B.; Datta, R.; Kim, D.H.; Todorov, N.D.; Pachauri, N.; Gupta, A. Raman studies of cation distribution and thermal stability of epitaxial spinel NiCo₂O₄ films. *J. Appl. Phys.* **2013**, *114*, 033514. [CrossRef]
26. Haenen, J.G.D.; Visscher, W.; Barendrecht, E.J. Oxygen Evolution on NiCo₂O₄ Electrodes. Ph.D. Thesis, Eindhoven University of Technology, Eindhoven, The Netherlands, 1985. [CrossRef]
27. Chang, T.-C.; Lu, Y.-T.; Lee, C.-H.; Gupta, J.K.; Hardwick, L.J.; Hu, C.-C.; Chen, H.-Y.T. The Effect of Degrees of Inversion on the Electronic Structure of Spinel NiCo₂O₄: A Density Functional Theory Study. *ACS Omega* **2021**, *6*, 9692–9699. [CrossRef]
28. Asano, K.; Ohnishi, C.; Iwamoto, S.; Shioya, Y.; Inoue, M. Potassium-doped Co₃O₄ catalyst for direct decomposition of N₂O. *Appl. Catal. B Environ.* **2008**, *78*, 242–249. [CrossRef]
29. Chromcakova, Z.; Obalova, L.; Kovanda, F.; Legut, D.; Titov, A.; Ritz, M.; Fridrichova, D.; Michalik, S.; Kustrowski, P.; Jiráková, K. Effect of precursor synthesis on catalytic activity of Co₃O₄ in N₂O decomposition. *Catal. Today* **2015**, *257*, 18–25. [CrossRef]

30. Wang, X.Y.; Wen, W.; Mi, J.X.; Li, X.X.; Wang, R.H. The ordered mesoporous transition metal oxides for selective catalytic reduction of NO_x at low temperature. *Appl. Catal. B-Environ.* **2015**, *176–177*, 454–463. [[CrossRef](#)]
31. Wang, Z.; Guo, P.; Cao, S.; Chen, H.; Zhou, S.; Liu, H.; Wang, H.; Zhang, J.; Liu, S.; Wei, S.; et al. Contemporaneous inverse manipulation of the valence configuration to preferred Co²⁺ and Ni³⁺ for enhanced overall water electrocatalysis. *Appl. Catal. B* **2021**, *284*, 119725. [[CrossRef](#)]
32. Grzybek, G.; Wójcik, S.; Legutko, P.; Grybo's, J.; Indyka, P.; Leszczynski, B.; Kotarba, A.; Sojka, Z. Thermal stability and repartition of potassium promoter between the support and active phase in the K-Co_{2.6}Zn_{0.4}O₄/α-Al₂O₃ catalyst for N₂O decomposition: Crucial role of activation temperature on catalytic performance. *Appl. Catal. B Environ.* **2017**, *205*, 597–604. [[CrossRef](#)]
33. Grzybek, G.; Stelmachowski, P.; Gudyka, S.; Duch, J.; Cmil, K.; Kotarba, A.; Sojka, Z. Insights into the twofold role of Cs doping on deN₂O activity of cobalt spinel catalyst—Towards rational optimization of the precursor and loading. *Appl. Catal. B Environ.* **2015**, *168–169*, 509–514. [[CrossRef](#)]
34. Zabilsky, M.; Erzhavets, B.; Dzhinovich, P.; Pintar, A. Ordered mesoporous CuO–CeO₂ mixed oxides as an effective catalyst for N₂O decomposition. *J. Chem. Eng.* **2014**, *254*, 153–162. [[CrossRef](#)]
35. Piskorz, W.; Zasada, F.; Stelmachowski, P.; Kotarba, A.; Sojka, Z. Decomposition of N₂O over the surface of cobalt spinel: A DFT account of reactivity experiments. *Catal. Today* **2008**, *137*, 418–422. [[CrossRef](#)]
36. Franken, T.; Palkovits, R. Investigation of potassium doped mixed spinels Cu_xCo_{3–x}O₄ as catalysts for an efficient N₂O decomposition in real reaction conditions. *Appl. Catal. B Environ.* **2015**, *176–177*, 298–305. [[CrossRef](#)]
37. Amrousse, R.; Tsutsumi, A.; Bachar, A.; Lahcene, D. N₂O catalytic decomposition over nano-sized particles of Co-substituted Fe₃O₄ substrates. *Appl. Catal. A Gen.* **2013**, *450*, 253–260. [[CrossRef](#)]

Disclaimer/Publisher's Note: The statements, opinions and data contained in all publications are solely those of the individual author(s) and contributor(s) and not of MDPI and/or the editor(s). MDPI and/or the editor(s) disclaim responsibility for any injury to people or property resulting from any ideas, methods, instructions or products referred to in the content.